Real-Time Reduced Steady-State Model Synthesis of Active Distribution Networks Using PMU Measurements

Farhan Mahmood, *Student Member, IEEE*, Hossein Hooshyar, *Member, IEEE*, Jan Lavenius, *Student Member, IEEE*, Ali Bidadfar, *Member, IEEE*, Per Lund, *Senior Member, IEEE*, and Luigi Vanfretti, *Senior Member, IEEE*

***Abstract*—Due to the increase of generation sources in distribution networks, it is becoming very complex to develop and maintain models of these networks. Network operators need to determine reduced models of distribution networks to be used in grid management functions. This paper presents a novel method that synthesizes steady-state models of unbalanced active distribution networks with the use of dynamic measurements (time series) from phasor measurement units (PMUs). Since phasor measurement unit (PMU) measurements may contain errors and bad data, this paper presents the application of a Kalman filter technique for real-time data processing. In addition, PMU data capture the power system's response at different time-scales, which are generated by different types of power system events; the presented Kalman filter has been improved to extract the steady-state component of the PMU measurements to be fed to the steady-state model synthesis application. Performance of the proposed methods has been assessed by real-time hardware-in-the-loop simulations on a sample distribution network.**

***Index Terms*—Active distribution network, Kalman filter (KF), model synthesis, PMU.**

NOMENCLATURE

TSO	Transmission System Operator.
SSMS	Steady State Model Synthesis.
PMU	Phasor Measurement Unit.
KF	Kalman Filter.
HIL	Hardware-in-the-Loop.
CRIO	Compact Reconfigurable Input Output.
S3DK	Statnett Syncrophasor Development Kit.
REI	Radial Equivalent and Independent.
LTC	Load Tap Changer.
FIR	Finite Impulse Response.
KVL	Kirchhoff's Voltage Law.

Manuscript received August 31, 2015; revised December 30, 2015 and April 22, 2016; accepted August 12, 2016. Date of publication August 24, 2016; date of current version January 20, 2017. This work was supported in part by the FP7 IDE4L project funded by the European Commission, in part by the STandUp for Energy Collaboration Initiative, and in part by Statnett SF, the Norwegian TSO. Paper no. TPWRD-01217-2015.

F. Mahmood, H. Hooshyar, J. Lavenius, and A. Bidadfar are with the KTH Royal Institute of Technology, Stockholm 114 28, Sweden (e-mail: farhanm@kth.se; hosseinh@kth.se; janlav@kth.se; Bidadfar@kth.se).

P. Lund is with the Energinet.dk, Fredericia DK-7000 Denmark (e-mail: plu@energinet.dk).

L. Vanfretti is with the KTH Royal Institute of Technology, Stockholm 114 28, Sweden, and also with the Statnett SF, Oslo 0484, Norway (e-mail: luigi.vanfretti@statnett.no).

Color versions of one or more of the figures in this paper are available online at http://ieeexplore.ieee.org.

Digital Object Identifier 10.1109/TPWRD.2016.2602302

I. INTRODUCTION

WITH the increase of renewable generation sources in the distribution networks, it is becoming more and more complex to develop and maintain models of these networks. Currently, most TSOs are only able to determine reduced models of limited portions of distribution networks including aggregated production models based on different distributed production technologies (wind, solar, hydro and thermal), to be used in their grid management functions [1]. This is due to the lack of network observability (too few measurements at the distribution level), insufficient network modeling information, and challenges with model information management that are coupled with computational issues when handling larger and larger models.

A. Motivation

Current methods used by TSOs to determine reduced models require a detailed model of the network to be reduced [2] and often make assumptions, such as pure loads, that are no longer valid for active distribution networks with the increased generation sources at lower voltage levels. In some cases, detailed modeling of a few portions of distribution networks, where there are voltage instabilities issues, is performed. However, the models are updated yearly and cannot be updated automatically [3]. PMU measurements from multiple locations in the distribution network can be exploited to be used for model synthesis of the distribution network.

However, PMU measurements are polluted with noise, outliers, and missing samples. Thus, cannot be directly fed to an application without adequate processing. Moreover, measurements obtained from PMUs during different events in power systems contain different signal features at different time scales. Hence they contain features of different types of power system dynamics. Not all PMU applications need the same type of signal. For steady state applications, like the SSMS application, the presence of oscillations adversely impacts the performance of the application [4]. Therefore, both bad data and oscillations should be filtered out from the PMU measurements before they can be fed to the application.

B. Literature Review

Steady state model synthesis of power system has been investigated in the past [5]–[8], mainly focusing on transmission systems where distribution networks represented by pure loads. The synthesized models, including only positive sequence networks, may not be used to represent unbalanced systems such as distribution networks. In [5], the Radial Equivalent and Independent (REI) equivalents are presented and in [6] reduced equivalent models are derived with LTC Transformers. Note that in both [5] and [6] reduced models are derived assuming that the detailed model of the system is available, which is uncommon (particularly for distribution networks) and their application for real-time model synthesis is not considered. In [9] and [10], the topology of the system is not known, but equivalents are calculated based on state estimation techniques. In [11] and [12], Ward equivalents are proposed. The issue with these equivalents is that the physical behavior of the internal system is accurate whereas the behavior of the external system is approximated, hence limiting their ability to retain the characteristics of the entire system. The methods, proposed in [7] and [8], can use real-time PMU measurements, making them suitable for real-time applications; however, they are restricted to acquire PMU measurements from a single location, making them unable to synthesize models for multiple sections of power networks. Hence, there is clearly a need to develop a method that performs model synthesis in real-time for multiple sections of unbalanced distribution networks.

The application of filters in state estimation using PMU data has been extensively discussed in [4], [13], and [14]. In [4] a method for extracting the steady state of input PMU data is presented using FIR and Median Filters. However, important aspects of dealing with noise, outliers and replacing missing data from the PMU measurements are not considered. Furthermore, the method has been discussed only for offline applications. In [13], an optimal assessment of the process noise covariance matrix Q on the accuracy of state estimation is made. A two stage KF approach is presented in [14] to simultaneously estimate the static and dynamic state. Both of these methods focus on state estimation using KF and are not suitable to extract steady state components from input PMU data. Therefore, a method is required to perform both data processing and extraction of steady state components from input PMU data in real-time.

C. Paper Contributions

This paper presents an application that performs real-time SSMS for multiple sections of unbalanced distribution networks by acquiring real-time measurements from multiple PMUs. The proposed approach is generic and can be applied to any section of a distribution network with any feeder configuration, generation sources or load types. Although having more PMUs provides better observability and allows the SSMS application to determine more detailed models, the developed SSMS application does not put any requirement in terms of the number of installed PMUs.

In addition, the paper presents the application of a Kalman Filter technique for PMU data processing. The Kalman Filter presented herein extracts the quasi-steady state component in PMU measurements and feeds them to the SSMS application. The method is capable of filtering noise, compensating for missing data and removing the outliers in PMU signals.

The paper begins by explaining the Kalman Filter application and its performance in Section II. In Section III, the developed SSMS method is discussed. Section IV describes the HIL real-time simulation setup used to assess the performance of the developed SSMS application. Section V presents the results from illustrative examples conducted using developed SSMS application. Conclusions are drawn in Section VI.

II. PMU Measurement Data Processing

PMU data is polluted with noise, outliers and missing samples. It also includes features of different types of power system dynamic response. Therefore adequate data processing is required to curate PMU data and to extract the quasi-steady state components of the PMU data before it can be fed to the SSMS application.

A. The Kalman Filter (KF)

A linear discrete time controlled process is assumed to have linear stochastic process and measurement equations as below:

$$\begin{aligned} \boldsymbol{x}_k &= \boldsymbol{A}\boldsymbol{x}_{k-1} + \boldsymbol{B}\boldsymbol{u}_k + \boldsymbol{w}_{k-1} \\ \boldsymbol{z}_k &= \boldsymbol{H}\boldsymbol{x}_k + \boldsymbol{v}_k \end{aligned} \tag{1}$$

where $\boldsymbol{x}$ is the state vector, $\boldsymbol{z}$ is the measurement vector, $\boldsymbol{A}$ is the n x n matrix that relates the state at previous time step k-1 to the state at current step k, which is assumed to be constant in each iteration, $\boldsymbol{B}$ is the control input which relates input u to the state $\boldsymbol{x}$ and $\boldsymbol{H}$ is the m x n matrix which relates state $\boldsymbol{x}_k$ to the measurements $\boldsymbol{z}_k$. The process noise $\boldsymbol{\omega}_k$ and measurement noise $\boldsymbol{v}_k$ are assumed to be two mutually independent random variables with normal probably distributions

$$\begin{aligned} p(\boldsymbol{w}) &\sim N(0, \boldsymbol{Q}) \\ p(\boldsymbol{v}) &\sim N(0, \boldsymbol{R}) \end{aligned} \tag{2}$$

where $\boldsymbol{Q}$ is the process noise covariance matrix and $\boldsymbol{R}$ is the measurement noise covariance matrix. These two matrices are usually constant but can be updated at each time step. The KF can be divided into two parts as below.

1) Time Update Equations (Prediction): The time update equations are responsible of projecting forward (in time) the previous state $\hat{\boldsymbol{x}}_{k-1}$ and the error covariance estimate $\boldsymbol{P}_{k-1}$ to obtain the a priori state estimates $\hat{\boldsymbol{x}}_k$ and the a priori error covariance estimate $\boldsymbol{P}_k^-$ for the next step k:

$$\begin{aligned} \hat{\boldsymbol{x}}_k^- &= \boldsymbol{A}\hat{\boldsymbol{x}}_{k-1}^- + \boldsymbol{B}\boldsymbol{u}_{k-1} \\ \boldsymbol{P}_k^- &= \boldsymbol{A}\boldsymbol{P}_{k-1}\boldsymbol{A}^T + \boldsymbol{Q} \end{aligned} \tag{3}$$

2) Measurements Update Equations (Correction): Measurement update equations are responsible for feedback by incorporating a new measurement $\boldsymbol{z}_k$ into the a priori estimate to

obtain an improved a posteriori estimate:

$$\begin{aligned} \boldsymbol{K}_k &= \boldsymbol{P}_k^- \boldsymbol{H}^T (\boldsymbol{H}\boldsymbol{P}_k^- \boldsymbol{H}^T + \boldsymbol{R})^{-1} \\ \hat{\boldsymbol{x}}_k &= \hat{\boldsymbol{x}}_k^- + \boldsymbol{K}_k (\boldsymbol{z}_k - \boldsymbol{H}\hat{\boldsymbol{x}}_k^-) \\ \boldsymbol{P}_k &= (\boldsymbol{I} - \boldsymbol{K}_k \boldsymbol{H}) \boldsymbol{P}_k^- \end{aligned} \tag{4}$$

where $\boldsymbol{K}$ is an n x m matrix known as the Kalman gain matrix, $\boldsymbol{z}_k$ is the actual measurement at step k, $H\hat{x}_k^-$ is the predicted measurement, $\hat{x}_k$ is the a posteriori estimate which is a linear combination of an a priori estimate $\hat{x}_k^-$ and a weighted difference between $\boldsymbol{z}_k$ and $H\hat{x}_k^-$.

The accuracy of a Kalman Filter output is influenced by the measurement and process noise covariance matrices, i.e., $\boldsymbol{R}$ and $\boldsymbol{Q}$ [9]. Therefore these two parameters can be exploited in a proper way to perform bad data processing and also extracting the proper signal feature of the PMU data.

B. The Modified KF Algorithm

$\boldsymbol{R}$ and $\boldsymbol{Q}$ can be updated in real-time to perform both bad data handling and to extract the steady state components from PMU data. As only the quasi-steady state components of the true state are of interest, any oscillations appearing in the measured signal are treated as bad data. $\boldsymbol{R}$ will be updated depending upon the quality of the measurements to filter out the bad data and extract the steady state component. $\boldsymbol{Q}$ will be updated to treat the unmodeled process noise which is, in our case, any change in the steady state value of the measured signal. This is because the process model, $\boldsymbol{A}$, is set to the unity matrix, $\boldsymbol{I}$, in order to force the output of the KF to settle at its steady state value.

The starting point of the proposed method relies on the concepts of *Innovation* ($\boldsymbol{I}_{nov}$) and *Residue* ($\boldsymbol{I}_{res}$), mentioned in [14], in order to detect and differentiate between the bad data and the process noise.

$$\begin{aligned} \boldsymbol{I}_{nov} &= (\boldsymbol{z}_k - \boldsymbol{H}\hat{\boldsymbol{x}}_k^-) \\ \boldsymbol{I}_{res} &= (\boldsymbol{z}_k - \boldsymbol{H}\hat{\boldsymbol{x}}_k) \end{aligned} \tag{5}$$

where $\boldsymbol{I}_{nov}$ has a normal probability density function and covariance $\boldsymbol{S}_k$ referred as *Innovation Covariance* which is calculated as:

$$\boldsymbol{S}_k = (\boldsymbol{H}\boldsymbol{P}_k^- \boldsymbol{H}^T + \boldsymbol{R}) \tag{6}$$

Note that the mean value of $\boldsymbol{I}_{nov}$ is normally zero, however in abnormal conditions, i.e., there exists some process noise or bad data in the measurements, the mean value can shift such that the normalized innovation, described in (7), will exceed a predetermined threshold value, τQ.

$$\boldsymbol{I}_{nov-norm} = \frac{|I_{nov}|}{\sqrt{S_k}} \tag{7}$$

Similarly, $\boldsymbol{I}_{res}$ has a normal probability density function and covariance $\boldsymbol{T}_k$ referred to as *Residual Covariance* that can be calculated as:

$$\boldsymbol{T}_k = \boldsymbol{R}\boldsymbol{S}_k^{-1}\boldsymbol{R} \tag{8}$$

Again, the mean value of $\boldsymbol{I}_{res}$ is normally zero, however in the presence of bad data, the mean value can shift such that the normalized residue, described in (9), will exceed a pre-determined threshold value, τ_{R}. Note that the process noise does not affect $\boldsymbol{I}_{res-norm}$. It is also worth noting that, in contrast to [14], we are using two separate threshold values for $\boldsymbol{I}_{nov-norm}$ and $\boldsymbol{I}_{res-norm}$ in order to have a degree of freedom in differentiating between the process noise and the bad data.

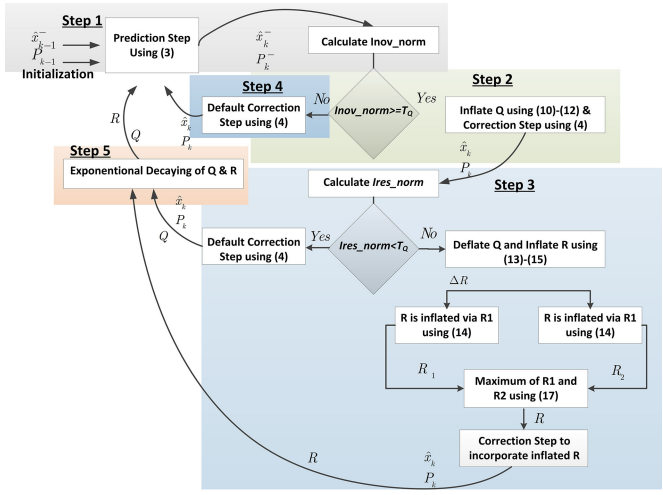

Fig. 1. Flowchart of the modified KF algorithm.

$$\boldsymbol{I}_{res-norm} = \frac{|\boldsymbol{I}_{res}|}{\sqrt{\boldsymbol{T}_k}} \tag{9}$$

For simplicity the time step k will be omitted from now on.

Note that as a general rule in KF methods, inflating $\boldsymbol{Q}$ leads to less dependence on the process model, i.e., matrix $\boldsymbol{A}$, and inflating $\boldsymbol{R}$ leads to less dependence on the measurements.

Algorithm:

Fig. 1 shows the flowchart of the proposed algorithm. The different steps of the algorithm are elaborated below:

1) Start the prediction step. Afterwards, calculate $\boldsymbol{I}_{nov-norm}$
2) If $\boldsymbol{I}_{nov-norm} \geq \tau_Q$, it indicates that there exists either process noise or bad data in the measurements that has caused $\boldsymbol{I}_{nov-norm}$ to exceed τ_{Q}. Assume that the problem is originating from the process noise, so reduce $\boldsymbol{I}_{nov-norm}$ back to τ_{Q} through inflating $\boldsymbol{Q}$ by $\Delta\boldsymbol{Q}$, as shown in equations (10)–(12).

$$\begin{aligned} \boldsymbol{I}_{nov-norm} &= \frac{|\boldsymbol{I}_{nov}|}{\sqrt{\boldsymbol{S}+\boldsymbol{\Delta S}}} = \tau_Q \Rightarrow \boldsymbol{\Delta S} \\ &= \left[\frac{|\boldsymbol{I}_{nov}|}{\tau_Q}\right]^2 - \boldsymbol{S} \end{aligned} \tag{10}$$

$$\boldsymbol{\Delta S} = \boldsymbol{H}\left(\boldsymbol{\Delta P}^{\cdot}\right)\boldsymbol{H}^T \Rightarrow \boldsymbol{\Delta P}^{\cdot} = \boldsymbol{H}^{-1}\left(\boldsymbol{\Delta S}\right)\left(\boldsymbol{H}^T\right)^{-1} \tag{11}$$

$$\boldsymbol{\Delta Q} = \boldsymbol{\Delta P}\boldsymbol{H}^- \Rightarrow \boldsymbol{Q}_{\inf} = \boldsymbol{Q} + \boldsymbol{\Delta Q} \tag{12}$$

3) In this step, calculate $\boldsymbol{I}_{res-norm}$ considering the inflated $\boldsymbol{Q}$. If $\boldsymbol{I}_{res-norm} < \tau_R$, it means that the assumption in step 1 is correct, otherwise it indicates that the problem is caused by the bad data in the measurements. So this requires to deflate $\boldsymbol{Q}$ back to its original value and instead, inflate $\boldsymbol{R}$ such that $\boldsymbol{I}_{nov-norm}$ and $\boldsymbol{I}_{res-norm}$

are reduced back to τ_{Q} (through (13) and (14)) and τ_{R} (through (15) and (16)), respectively. Note that as (16) is a nonlinear equation, it must be solved numerically, e.g., $\boldsymbol{R}_2$ can be increased iteratively starting from $\boldsymbol{R}$ until $\boldsymbol{R}_2(cte+\boldsymbol{R}_2)^{-1}\boldsymbol{R}_2 \geq \boldsymbol{T}_2$. Finally note that, as shown in (17), the inflated R is equal to the maximum of $\boldsymbol{R}_1$ and $\boldsymbol{R}_2$.

$$\boldsymbol{I}_{nov-norm} = \frac{|\boldsymbol{I}_{nov-norm}|}{\sqrt{\boldsymbol{S}+\boldsymbol{\Delta S}}} = \tau_Q \Rightarrow$$

$$\boldsymbol{\Delta S} = \left[\frac{|\boldsymbol{I}_{nov}|}{\tau_Q}\right]^2 - \boldsymbol{S} \tag{13}$$

$$\boldsymbol{\Delta R} = \boldsymbol{\Delta S} \Rightarrow \boldsymbol{R}_1 = \boldsymbol{R} + \boldsymbol{\Delta R} \tag{14}$$

$$\boldsymbol{I}_{res-norm} = \frac{|\boldsymbol{I}_{res}|}{\sqrt{\boldsymbol{T}_2}} = \tau_R \Rightarrow \boldsymbol{T}_2 = \left[\frac{|\boldsymbol{I}_{res}|}{\tau_R}\right]^2 \tag{15}$$

$$\boldsymbol{T}_2 = \boldsymbol{R}_2(cte+\boldsymbol{R}_2)^{-1}\boldsymbol{R}_2 \tag{16}$$

$$\boldsymbol{R}_{inf} = \max(\boldsymbol{R}_1, \boldsymbol{R}_2) \tag{17}$$

4) The correction step is performed using the inflated $\boldsymbol{Q}$ or $\boldsymbol{R}$. If neither $\boldsymbol{Q}$ nor $\boldsymbol{R}$ is inflated, the method uses the original $\boldsymbol{Q}$ and $\boldsymbol{R}$.
5) The inflated $\boldsymbol{Q}$ or $\boldsymbol{R}$ is deflated using an exponential decaying factor in the beginning of the next execution to treat temporary problems e.g., Outliers etc.

Equations (7), (9), (10), (13) and (15) compute a scaled array. To scale the array, the division is computed at the *k*-th iteration, for all elements in the *Ix* array $(1:\mathrm{n},1)_{\mathrm{k}}$ (where n = number of variables, and $x = \{nov,\ res\}$) over a single element $(p,q)_k$ of matrix (*S* or *T*). Therefore, results in the *Ix-norm* array.

C. Performance of the Modified KF

The modified KF method has been applied on PMU data from HIL experiment as shown in Fig. 2. The figure shows the voltage magnitude and angle in a distribution system where a load, is connected at t = 5 s and disconnected at t = 75 s. As the figure shows, outliers are generated at the switching time instants. Also, the signals include oscillations due to random consumption variations of the connected load.

In this experiment, τ_Q and τ_R have been set to 1 and 0.5, respectively. Depending upon the value of $\boldsymbol{S}_k$ and $\boldsymbol{T}_k$, τ_Q and τ_R set different limits on the allowed variation of $\boldsymbol{I}_{nov}$ and $\boldsymbol{I}_{res}$, before the algorithm detects bad data or a change in the steady state value.

As Fig. 2 shows, the modified KF filters out the system's dynamic response (oscillations), as well as outliers. The extracted steady state component of the signals (shown in red) will be fed as the input to the SSMS application, which will be discussed in the next section.

III. Steady State Model Synthesis

Using the output of the modified KF, reduced equivalent models of distribution networks can be synthesized. The model structure and parameters can be updated and sent to the TSOs in real-time. Hence, the models provide new valuable information to TSOs to improve their energy management functions.

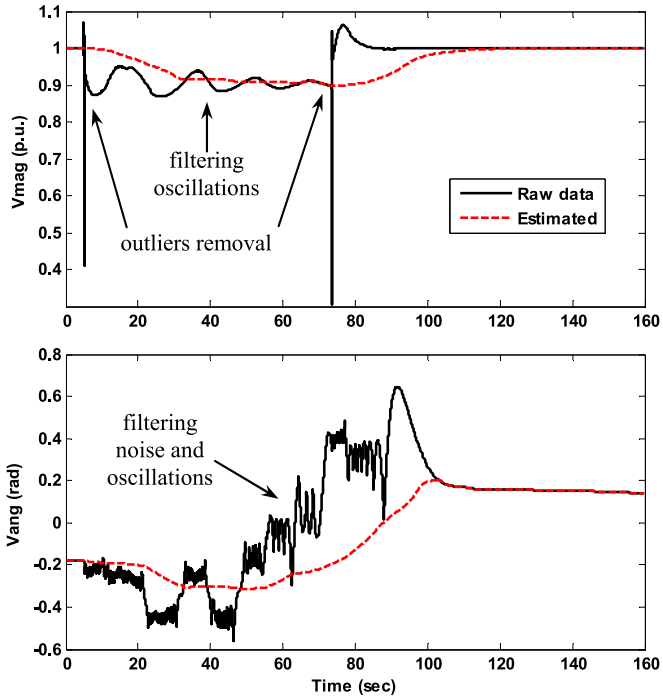

Fig. 2. Performance of the modified KF.

A. Problem Statement

TSOs need to determine reduced models of distribution networks to be used in their grid management functions and to have more insight over distribution networks. Currently, some TSOs are able to determine reduced models of limited portions of the distribution networks however the models are updated yearly. Also, available models have assumptions, such as pure loads, that are no longer valid for active distribution networks.

Assuming that PMU measurements are available at any single or more buses in a distribution network and they measure all three-phase voltage and current phasors, a three phase steady state equivalent model can be synthesized for the portion of the distribution network that is located between the installed PMUs. As the operating conditions of the system changes, the parameters of the equivalent model are updated accordingly.

B. Model Synthesis Based on Two PMU Measurement Points at the Distribution Network

Fig. 3 shows an arbitrary section of the distribution network, bounded by two buses with PMU measurements. As the figure shows, the bounded section may include any kind of feeder structure with an arbitrary combination of loads and generation sources. The three-phase voltage and line current synchrophasor measurements, provided by the PMUs, can be utilized to derive the reduced steady state model. As Fig. 3 depicts, the model consists of a parallel branch, including an impedance in series with a voltage source to represent the net balance of generation/load in the selected section, and two series impedance to represent

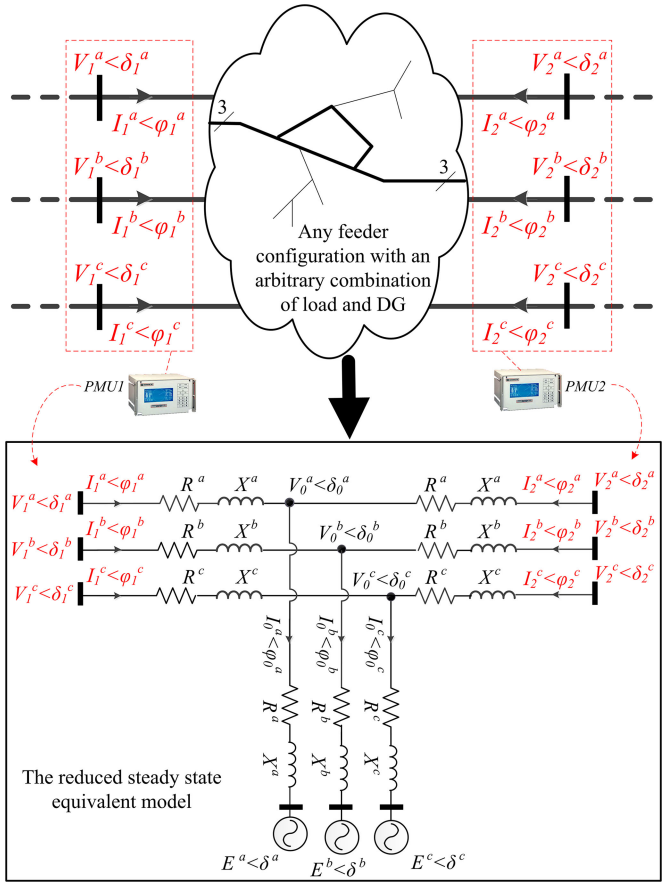

Fig. 3. Synthesized model based on two PMU measurement points.

the power loss in the feeders of the selected section. The model is synthesized in three phase to capture the unbalance between the three phases of the distribution network.

PMU measurement points provide three phase voltage and current phasors (shown in red in Fig. 3) which are the known entities in the model. The impedance of the series and parallel branches, and the magnitude and the angle of the voltage sources are the unknown parameters of the model.

Applying a KVL equation on phase 'a' of the series branch of the model yields (18).

$$V_1^a \angle \delta_1^a - V_2^a \angle \delta_2^a = (R^a + jX^a)\,(I_1^a \angle \varphi_1^a - I_2^a \angle \varphi_2^a) \quad (18)$$

Separating real and imaginary parts of (18) and converting them to rectangular form yields (19) and (20), resulting in a system of two linear equations with two unknowns.

Solving (19) and (20) gets the value of R^a and X^a.

$$V_{r1}^a - V_{r2}^a = R^a\,(I_{r1}^a - I_{r2}^a) - X^a\,(I_{i1}^a - I_{i2}^a) \quad (19)$$

$$V_{i1}^a - V_{i2}^a = R^a\,(I_{i1}^a - I_{i2}^a) + X^a\,(I_{r1}^a - I_{r2}^a) \quad (20)$$

where V_r^a, V_i^a, I_r^a, and I_i^a are the real and imaginary parts of the voltage and current phasors, respectively. Note that as indicated in Fig. 3, the model is assumed to have equal impedances in the series and in the parallel branches.

As $V_0^a \angle \delta_0^a = V_1^a \angle \delta_1^a - (R^a + jX^a) I_1^a \angle \varphi_1^a$ and $I_0^a \angle \varphi_0^a = I_1^a \angle \varphi_1^a + I_2^a \angle \varphi_2^a$, the voltage source of the parallel branch

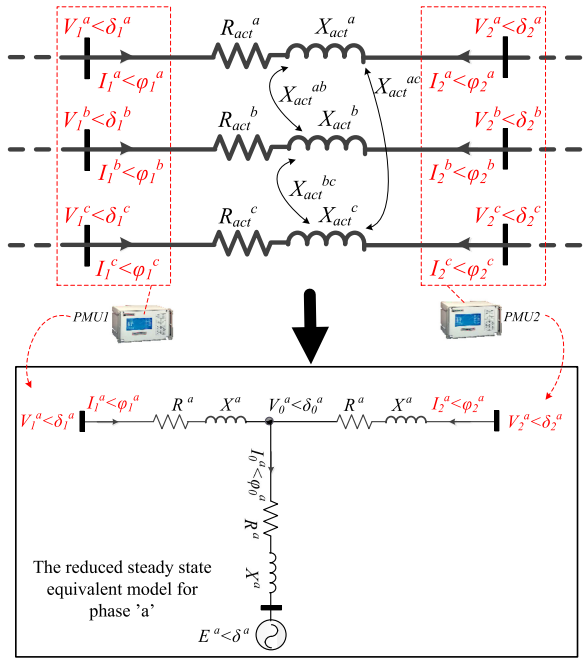

Fig. 4. Model synthesis for a three-phase branch with mutual couplings.

can be obtained from (21).

$$E^a \angle \delta^a = V_0^a \angle \delta_0^a - (R^a + jX^a)\, I_0^a \angle \varphi_0^a \quad (21)$$

Separating real and imaginary parts of (21) and converting them to rectangular form yields (22) and (23), which can be solved to obtain the value of E^a and δ^a.

$$E_r^a = V_{r0}^a - R^a I_{r0}^a + X^a I_{i0}^a \quad (22)$$

$$E_i^a = V_{i0}^a - R^a I_{i0}^a - X^a I_{r0}^a \quad (23)$$

where E_r^a and E_i^a are the real and imaginary parts of the voltage source phasor, respectively.

Following the same logic, explained through equations (18)–(23), the parameters of the other phases, i.e., R^b, X^b, R^c, X^c, E^b, δ^b, E^c, and δ^c can be derived similarly.

Therefore, by utilizing the synchrophasor measurements, belonging to the same time instant (i.e., syncrophasor snapshot), the parameters of the model can be calculated through equations (18)–(23). Note that the calculated values are valid only for the specific time instant to which the measurements belong to. Hence, they should be updated in real-time by using the incoming real-time PMU measurements, which are processed by the KF.

An important implication of updating the parameters in real-time is that the synthesized model reproduces the voltage drop between the two PMU measurement points, i.e., $\vec{V}_1 - \vec{V}_2$, simultaneously. This means that the proposed model considers not only the voltage drop caused by the phase current but it also takes into account the induced voltage drop due to the mutual couplings between the phases. In order to clarify this matter, let's consider synthesizing phase 'a' of a simple branch, shown in Fig. 4. As the figure shows, the voltage drop across the branch can be derived from (24). Note that the subscript 'act' refers to

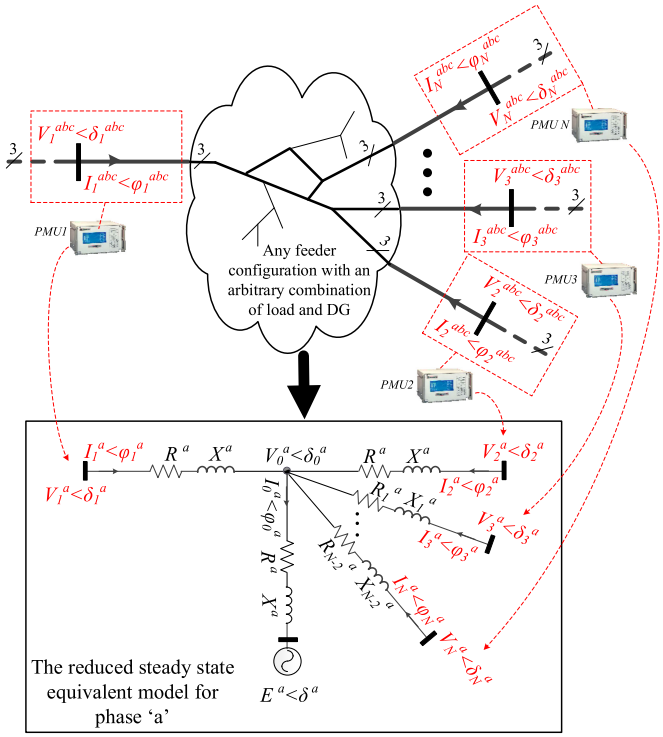

Fig. 5. Synthesized model based on '*N*' number of PMU measurement points.

the "actual value" of the parameters to differentiate them from the values in the synthesized model.

$$V_1^a\angle\delta_1^a - V_2^a\angle\delta_2^a = \left(R_{act}^a + jX_{act}^a\right)\left(I_1^a\angle\varphi_1^a - I_2^a\angle\varphi_2^a\right) + jX_{act}^{ab}\left(I_1^b\angle\varphi_1^b - I_2^b\angle\varphi_2^b\right) + jX_{act}^{ac}\left(I_1^c\angle\varphi_1^c - I_2^c\angle\varphi_2^c\right) \quad (24)$$

The voltage drop, derived in (24), can be calculated by (25) using the estimated model parameters.

$$V_1^a\angle\delta_1^a - V_2^a\angle\delta_2^a = \left(R^a + jX^a\right)\left(I_1^a\angle\varphi_1^a - I_2^a\angle\varphi_2^a\right) \quad (25)$$

By equating (24) and (25), the modeled impedance will be obtained as:

$$R^a + jX^a = \frac{\left(R_{act}^a + jX_{act}^a\right)\left(I_1^a\angle\varphi_1^a - I_2^a\angle\varphi_2^a\right) + jX_{act}^{ab}\left(I_1^b\angle\varphi_1^b - I_2^b\angle\varphi_2^b\right) + jX_{act}^{ac}\left(I_1^c\angle\varphi_1^c - I_2^c\angle\varphi_2^c\right)}{I_1^a\angle\varphi_1^a - I_2^a\angle\varphi_2^a} \quad (26)$$

which clearly shows that the calculated per phase impedance is a function of voltage drops caused by both the self- and the mutual impedances. For example, any change in $\vec{I}_2^b$ will affect the phase 'a' impedance $R^a + jX^a$ through the mutual impedance X_{act}^{ab}.

C. Model Synthesis Based on 'N' Number of PMU Measurement Points at the Distribution Network

The modeling approach, followed in the previous section, can be extended to model a portion of the distribution network that is bounded by multiple PMUs. Fig. 5 shows the model synthesis of phase 'a' of such a portion. As shown in the figure, addition of each PMU results in addition of an extra series branch to the synthesized model.

Equations (18)–(23) are still valid to determine the impedance of the parallel branch and the series branches between PMU1 and PMU2, i.e., $R^a + jX^a$, and also to determine the voltage source phasor $E^a < \delta^a$, except that $I_0^a\angle\varphi_0^a = \sum_{k=1}^{N} I_k^a\angle\varphi_k^a$.

The impedance of the other series branches, i.e., .., can be determined by (27).

$$V_1^a\angle\delta_1^a - V_k^a\angle\delta_k^a = \left(R^a + jX^a\right)I_1^a\angle\varphi_1^a - \left(R_{k-2}^a + jX_{k-2}^a\right)I_k^a\angle\varphi_k^a \quad (27)$$

where $k = 3, 4, ..., N$ representing the branch number. Separating real and imaginary parts of (27) and converting them to rectangular form yields two linear equation from which the two unknown, R_{k-2}^a and X_{k-2}^a, can be determined.

Note that, when applying this method, PMU1 and PMU2 are the two PMUs that have the smallest impedance between them among any other pair of the PMUs. This is to ensure that the impedances, to be calculated for the other series branches i.e., $R_{k-2}^a + jX_{k-2}^a$, do not become negative. Hence, in order to select the correct pair of PMUs as PMU1 and PMU2, the impedance $R + jX$ should be evaluated through equations (18) for any pair combination of the *N* PMUs. The two PMUs having the smallest $R + jX$ will be selected to be PMU1 and PMU2.

D. Model Synthesis Based on One PMU Measurement Point at the Distribution Network

For a single PMU measurement point, i.e., $N = 1$, the PMU has to be installed at the end of one of the distribution feeders. As Fig. 6 shows, the proposed method needs to utilize a single transmission level PMU, installed at the high voltage side of the point of common connection substation, so that the two PMUs, i.e., the transmission level PMU and the distribution level PMU bound the whole distribution network.

As indicated in Fig. 6, the synthesized model will be the same as a Thevenin equivalent model covering the whole distribution network starting from the transmission side of the substation, i.e., where the transmission level PMU is installed.

IV. HIL Real-Time Simulation Setup

This section describes the HIL real-time simulation setup in which the KF and SSMS method, developed in the previous sections are validated.

As shown in Fig. 7, two measurement locations have been specified on a grid model that is simulated by the OPAL-RT real-time simulator. The measured voltages and currents are fed to PMUs through the analogue output ports of the OPAL-RT simulator. As indicated in the figure, the PMUs used in this setup are Compact Reconfigurable IO systems (CRIO) from National Instruments Corporation, programmed with LabVIEW graphical programming tools to perform phasor calculations [15]. As the figure shows, the current signals are passed through the current amplifiers before being fed to the PMUs. Syncrophasors are then

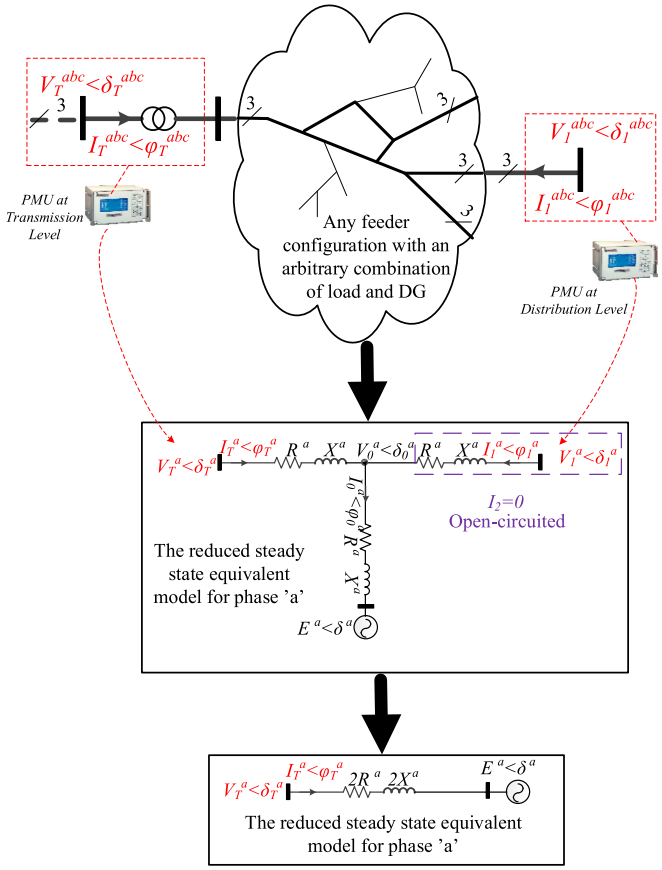

Fig. 6. Synthesized model based on one PMU at the distribution network.

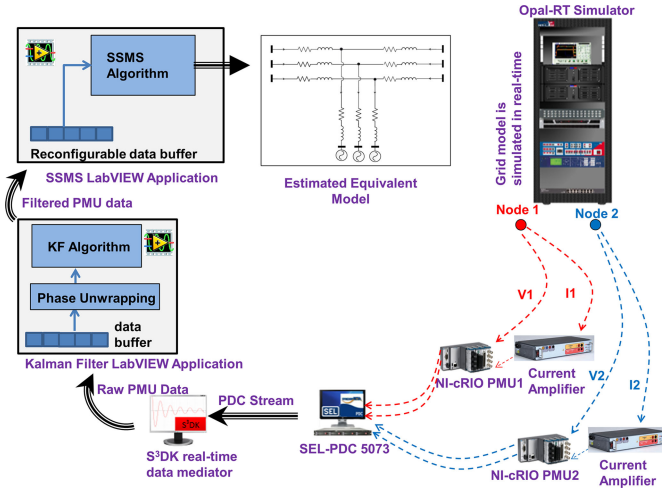

Fig. 7. HIL real-time simulation setup.

sent to a Phasor Data Concentrator (PDC) which streams the data over TCP/IP to a workstation computer holding Statnett's Synchrophasor Development Kit (S^{3}DK) [16], which provides a real-time data mediator that parses the PDC data stream and makes it available to KF application in the LabVIEW environment. The KF application is implemented based on the modified KF method, proposed in Section II.B. The output of the KF application is stored in a reconfigurable data buffer, from which

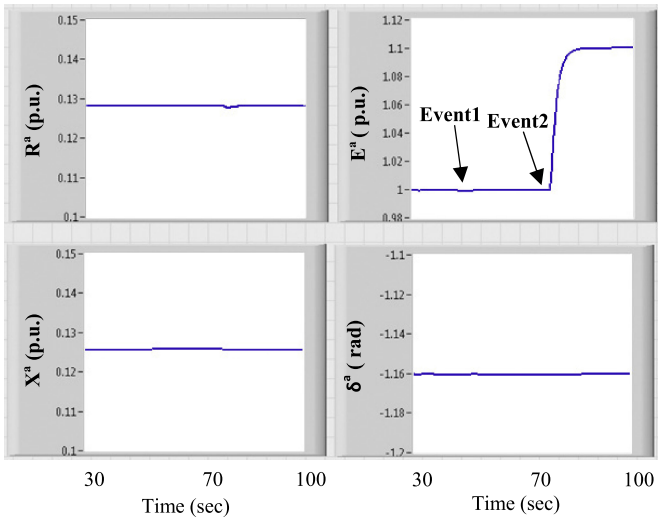

Fig. 8. Reproduction of the parameters of phase 'a' of the equivalent model by LabVIEW SSMS application (Example 1).

the SSMS application reads the data. The SSMS application estimates the unknown parameters of the proposed equivalent model and updates them in real-time.

V. Illustrative Examples

A. Example 1: Reproduction of the Equivalent Model Parameters in Real-Time

A simple equivalent model as shown in Fig. 3, is included in a power system model (not shown here) and is simulated for 100 s with known parameters to reproduce the values of the parameters by the SSMS application. Using the HIL setup, shown in Fig 7, the PMU measurements were available on both buses of the model. The true values of the parameters on phase 'a' of the model are $R^a = 0.128$ p.u., $X^a = 0.126$ p.u., $E^a = 1$ p.u., and $\delta^a = -1.1591$ rad. In this example, it has been assumed that there is no mutual coupling between the phases.

Two Events were created in the simulation: 1) A load of (0.2 + j0.1) p.u. is connected at t = 40 s in the right side of PMU2 (Event occurs outside the bounded section by the PMUs) and, 2) A step increment of 10% is introduced in E^a at t = 70 s (the Event occurs inside the bounded section by the PMUs). Fig. 8 shows the reproduced model parameters for phase 'a' of the model by the implemented SSMS application.

It is evident from Fig. 8 that for Event 1 there are no noticeable changes in the model parameters as it was outside the boundary of the two PMUs; whereas E^a is updated accordingly for Event 2 (see top right of Fig. 8).

B. Example 2: Incorporating the Effect of Mutual Inductances

In this example, it is shown how the existence of the mutual coupling between the phases will affect the estimated value of the model parameters.

For this example, three different models are simulated:

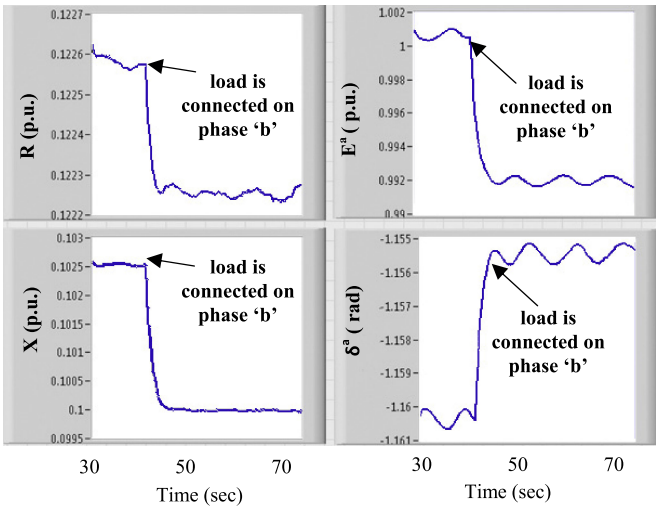

Fig. 9. Estimation of the parameters of phase 'a' of Model 2 (Example 2).

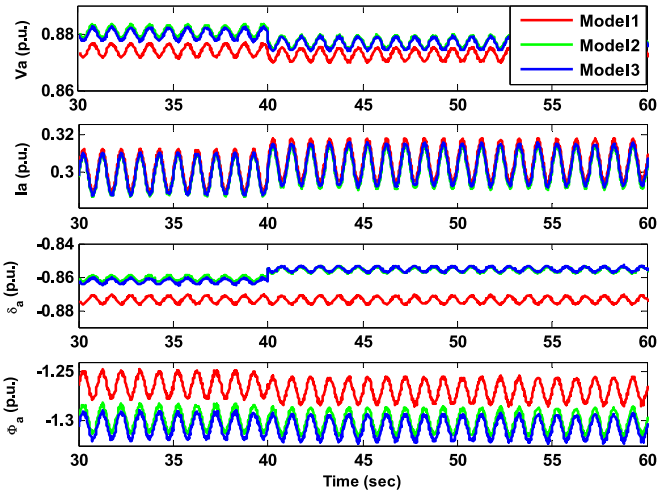

Fig. 10. Voltage and current phasor of PMU2 in Model 1, Model 2, and Model 3 (Example 2).

Model 1: Equivalent model without any mutual inductance between the phases (same as Example 1)

Model 2: Same as Model 1 with addition of mutual inductance between the phases. The values of the mutual inductances are $X^{ab} = 0.0066$ p.u., $X^{ac} = 0.0092$ p.u., and $X^{bc} = 0.0079$ p.u.

Model 3: The parameters of Model 2, estimated by the SSMS application, are inserted to an equivalent model, shown in Fig. 3. The voltages and currents at the PMU measurement points of Model 2 are then compared with those of the Model 3 for the purpose of validation. Note that Model 2 is the "true" model with mutual coupling whereas Model 3 is a synthesized model of Model 2.

Fig. 9 shows the estimated values of the parameters of phase 'a' of Model 2. As shown in the figure, the estimated values of the per phase parameters, i.e., R^a, X^a, E^a, and δ^a, are different from the real values due to the existence of the mutual coupling between the phases. Also, In order to better show the effect of mutual coupling, a load of $(0.2 + \text{j}0.1)$ p.u. is connected to phase 'b' at t = 40 s.

As shown in the figure, although the Event is taking place on phase 'b', it impacts the values of the parameters on phase 'a' due to the existence of the mutual coupling.

Fig. 10 compares the voltage and current magnitude and angles of PMU2 for all the three models. As shown in the figure, the voltage phasor is noticeably different if the effect of the mutual couplings is not considered (compare Model 1 with Model 2/Model 3). Also, the figure shows that Model 3 reproduces the voltage and current phasors of Model 2 quite accurately, which validates the accuracy of the parameters of Model 3 that is estimated by the SSMS application.

C. Example 3: Model Synthesis of a Sample Active Distribution Network

In this section, the SSMS application is applied on a sample active distribution network. The sample network has been

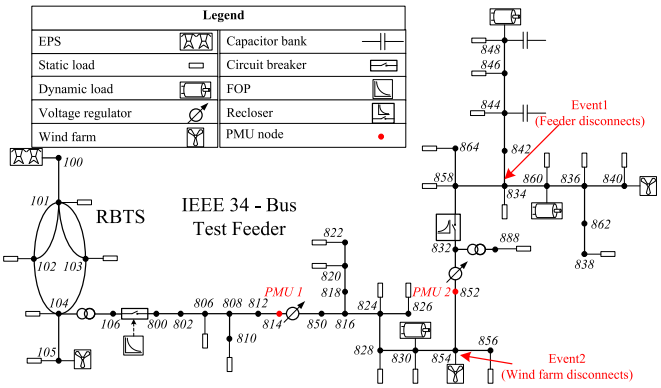

Fig. 11. Single-line diagram of the sample network.

adopted from an active distribution network model, presented in [17]. Fig. 11 depicts the single-line diagram of the sample network. PMU measurements were made available by connecting the Opal-RT simulator in HIL, similarly as in Fig. 7, on Node 814 and Node 852.

Two Events were created in the simulation: 1) A lateral MV feeder disconnects at Node 834 at t = 40 s, and 2). A wind farm generation of 1 MW (0.2 p.u.) disconnects at Node 854 at t = 70 s.

The equivalent model parameters for phase 'a', estimated by the SSMS application, are shown in Fig. 12. As the figure shows, the disconnection of the lateral feeder (Event 1) mainly impacts the value of R^a and X^a. This is because when the lateral feeder disconnects, the currents flowing through all phases of the main feeder reduce accordingly which, in turn, decreases the voltage drop induced on all phases through the mutual coupling. In case of Event 2, the disconnection of the wind farm, located inside the bounded section of the two PMUs, causes voltage to drop from 0.982 p.u. to 0.93 p.u.

In order to validate the equivalent model parameters, estimated by the SSMS application, the bounded section of the sample network has been replaced by an equivalent steady state

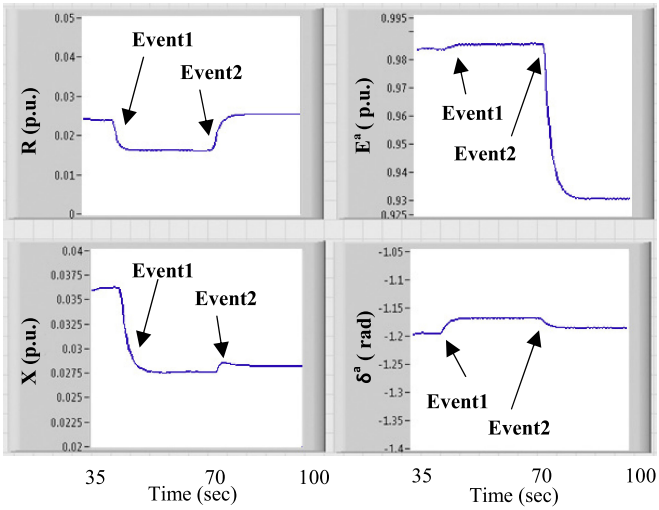

Fig. 12. Estimation of the parameters of phase 'a' of the sample network (Example 3).

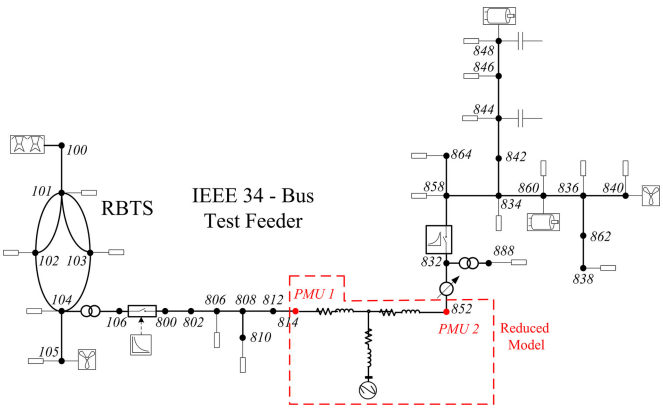

Fig. 13. Single-line diagram of the network with the equivalent model.

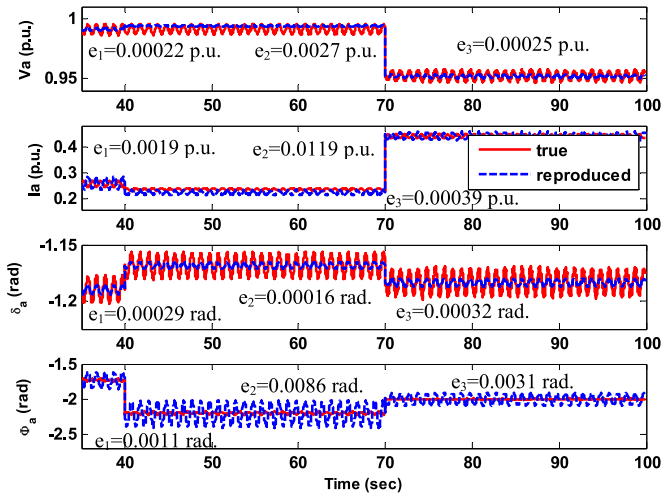

Fig. 14. True phasors versus reproduced phasors for PMU 1 (Example 3).

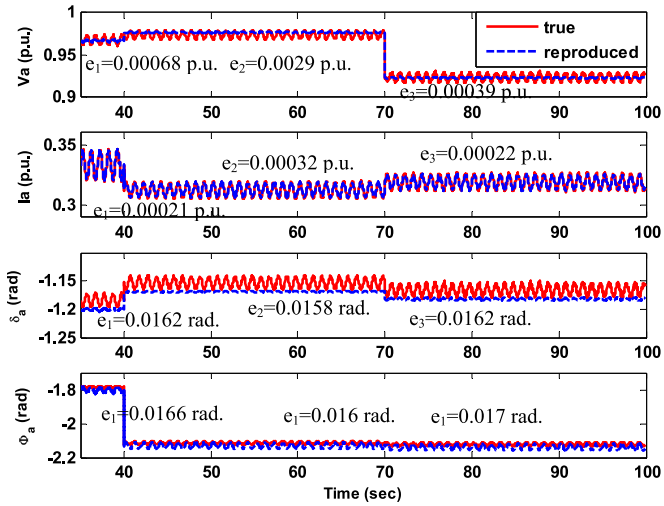

Fig. 15. True phasors versus reproduced phasors for PMU 2 (Example 3).

model, as shown in Fig. 13. The same Events, performed on the sample network, have been simulated on the network, shown in Fig. 13.

During the simulation, the parameters of the equivalent model have been updated.[1] Figs. 14 and 15 compare the voltage and current phasors, provided by PMU1 and PMU2 in the sample network, with those of the network containing the equivalent model. Note that the oscillations in the phasor signals are due to the sinusoidal variation embedded in the static load models of the simulated network. As the figure shows, the reproduced voltage and current phasors are quite similar to those of the sample network, which shows the validity of the developed SSMS application. In order to analyze the difference between the true values and the reproduced values, the mean error is calculated for each sections of the simulation i.e., e1 = before Event1, e2 = between Event 1 and Event 2, and e3 = after Event 2. The calculated errors are shown in Figs. 14 and 15.

As shown in the figures, for both PMUs, the maximum error of voltage magnitudes, current magnitudes, voltage angles, and current angles are 0.00068 p.u., 0.0119 p.u., 0.0162 rad., and 0.017 rad., respectively.

[1]The parameters are updated at the start of each Event and held constant up to the next Event.

VI. Conclusions and Future Works

This paper has presented an approach to perform steady state model synthesis (SSMS) in real-time for multiple sections of unbalanced distribution networks using synchronized phasor measurement data. An improved Kalman filtering technique in Section II is implemented for bad data handling and extracting steady state component of the PMU data to be fed to the SSMS application.

It has been shown that the proposed SSMS technique can produce accurate model for any feeder configuration located between the installed PMUs. If the system configuration changes, the parameters of the synthesized model will automatically update in real-time. Also, the updated parameters can be sent to TSOs in real-time to improve their energy management functions.

REFERENCES

[1] X. Cheng and T. J. Overbye, "PTDF-based power system equivalents," in *IEEE Trans. Power Syst.*, vol. 20, no. 4, pp. 1868–1876, Nov. 2005.

[2] J. H. Chow, Ed., *Power System Coherency and Model Reduction*. New York, NY, USA: Springer, 2013.

[3] North American Electric Reliability Corporation, "Power system model validation: A white paper by the NERC model validation task force of the transmission issues subcommittee," Atlanta, GA, USA, Dec. 2010.

[4] J. Tate and T. Overbye, "Extracting steady state values from phasor measurement unit data using FIR and median filters," in *Proc. IEEE Power Energy Soc. Power Syst. Conf. Expo.*, Seattle, WA, USA, 2009, 1–8.

[5] F. Milano and K. Srivastava, "Dynamic REI equivalents for short circuit and transient stability analyses," *Elect. Power Syst. Res.*, vol. 79, no. 6, pp. 878–887, Jun. 2009.

[6] G. B. Denegri, M. Invernizzi, and F. Milano, "Synthesis of an equivalent dynamic model for load areas with LTC transformers," in *Proc. IEEE Power Eng. Soc. Transm. Distrib. Conf. Expo.*, Atlanta, GA, USA, 2001, 641–646.

[7] M. Parniani, J. H. Chow, L. Vanfretti, B. Bhargava, and A. Salazar, "Voltage stability analysis of a multiple-infeed load center using phasor measurement data," in *Proc. IEEE Power Eng. Soc. Power Syst. Conf. Expo.*, Atlanta, GA, USA, 2006, 1299–1305.

[8] L. Vanfretti and F. R. S. Sevilla, "A three-layer severity index for power system voltage stability assessment using time-series from dynamic simulations," in *Proc. Innovat. Smart Grid Technol. Conf. Eur.*, Istanbul, Turkey, 2014, 1–5.

[9] K. Hongrae and A. Abur, "Enhancement of external system modeling for state estimation [power systems]," *IEEE Trans. Power Syst.*, vol. 11, no. 3, pp. 1380–1386, Aug. 1996.

[10] G. N. Korres, "A partitioned state estimator for external network modeling," *IEEE Trans. Power Syst.*, vol. 17, no. 3, pp. 834–842, Aug. 2002.

[11] S. Deckmann, A. Pizzolante, A. Monticelli, B. Stott, and O. Alsac, "Studies on power system load flow equivalencing," *IEEE Trans. Power App. Syst.*, vol. PAS-99, no. 6, pp. 2301–2310, Nov. 1980.

[12] F. C. Aschmoneit and J. F. Verstege, "An external system equivalent for on-line steady-state generator outage simulation," *IEEE Trans. Power App. Syst.*, vol. PAS-98, no. 3, pp. 770–779, May 1979.

[13] L. Zanni, S. Sarri, M. Pignati, R. Cherkaoui, and M. Paolone, "Probabilistic assessment of the process-noise covariance matrix of discrete Kalman filter state estimation of active distribution networks," in *Proc. Int. Conf. Probabilistic Meth. Appl. Power Syst.*, 2014, 1–6.

[14] J. Zhang, G. Welch, G. Bishop, and Z. Huang, "A two-stage Kalman filter approach for robust and real-time power system state estimation," *IEEE Trans. Sustain. Energy*, vol. 5, no. 2, pp. 629–636, Apr. 2014.

[15] P. Romano and M. Paolone, "Enhanced interpolated-DFT for synchrophasor estimation in FPGAs: Theory, implementation, and validation of a PMU prototype," *IEEE Trans. Instrum. Meas.*, vol. 63, no. 12, pp. 2824–2836, Dec. 2014.

[16] L. Vanfretti, V. H. Aarstrand, M. S. Almas, V. S. Peric, and J. O. Gjerde, "A software development toolkit for real-time synchrophasor applications," in *Proc. IEEE PowerTech*, 2013, 1–6.

[17] H. Hooshyar, F. Mahmood, L. Vanfretti, and M. Baudette, "Specification, implementation, and hardware-in-the-loop real-time simulation of an active distribution grid," *Sustain. Energy, Grids Netw.*, vol. 3, Sep. 2015, pp. 36–51.

Farhan Mahmood (S'12) received the M.Sc. degree in electrical power engineering from KTH Royal Institute of Technology, Stockholm, Sweden, in 2012, where he is currently working toward the Ph.D. degree in electric power and energy systems.

His research interest includes integration of renewable energy, real-time digital simulation of power systems, smart grids, and applications of PMU data for active distribution networks.

Hossein Hooshyar (S'00–M'14) received the Ph.D. degree in electrical engineering from North Carolina State University, Raleigh, NC, USA, in 2012.

Since 2013, he has been a Postdoctoral Associate with KTH Royal Institute of Technology, Stockholm, Sweden. His research interest includes digital simulation of power systems, integration of renewable energy resources, and applications of PMU data for smart grids.

Jan Lavenius (S'14) received the M.Sc. degree in electrical engineering from KTH Royal Institute of Technology, Stockholm, Sweden, in 2012 where he is currently pursuing the Ph.D. degree in electric power and energy systems.

His research interests include power system stability and control with a focus on voltage stability, and applications of PMU data in power system operation and control.

Ali Bidadfar (M'14) received the M.Sc. degree in electrical engineering from Tafresh University, Tafresh, Iran, in 2008 and is currently pursuing the Ph.D. degree in electrical engineering from Amirkabir University of Technology (AUT), Tehran, Iran.

Since 2013, he has been a Research Engineer at KTH Royal Institute of Technology, Stockholm, Sweden. His main research interests include high-voltage direct-current transmission links, power system dynamics and stability, and control systems.

Per Lund (SM'02) received the Ph.D. degree in industrial research from the Danish Academy of Technical Sciences, Lyngby, Denmark, in 1985.

He has been with the national Danish transmission system operator Energinet.dk since 2005. In addition to his deep involvement in major smart grid activities of Energinet.dk, he was the Chief Architect and technically responsible for the Cell Controller Pilot Project. He is heavily involved in the development of a phasor measurement unit based wide area monitoring and control system for Energinet.dk. He is currently a Chief Engineer in the Network Planning Department.

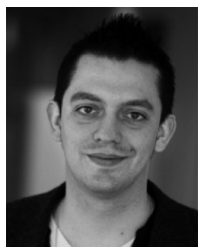

Luigi Vanfretti (S'03–M'10–SM'13) received the Ph.D. degree in electric power engineering from Rensselaer Polytechnic Institute, Troy, NY, USA, in 2009.

He became an Assistant Professor with the KTH Royal Institute of Technology, Stockholm, Sweden, in 2010 and has been a tenured Associate Professor since 2013. He is currently a Special Advisor at the R&D Division, Statnett SF, the Norwegian transmission system operator, where he previously held different internal positions during 2013–2014, and served as an external advisor during 2011–2012. He is an Advocate and Evangelist for free/libre software. His research interests include the general area of cyber-physical power system dynamics and the development of PMU data applications.